

The maximum error in surface pressure with respect to a mean drawn through Cleary's experimental data is less than 12%, and the computed shock shapes differ from one another by less than 5%.

References

- ¹ Moretti, G. et al., "Three-Dimensional Inviscid Flow About Supersonic Blunt Cones at Angle of Attack," SC-CR-68-3728, Sept. 1968, Sandia Corp., Albuquerque, N. Mex.
- ² Sanlorenzo, E. A. et al., "Flow Field Analysis of Reentry Configurations by a General Three-Dimensional Method of Characteristics," GASL-TR-247, Vol. III, April 1962, General Applied Science Lab., Westbury, N. Y.
- ³ Rakich, J. V. and Cleary, J. W., "Theoretical and Experimental Study of Supersonic Steady Flow Around Inclined Bodies of Revolution," AIAA Paper 69-187, New York, 1969.
- ⁴ Cleary, J. W., "An Experimental and Theoretical Investigation of the Pressure Distribution and Flow Fields of Blunted Cones at Hypersonic Mach Numbers," TN-D-2969, 1965, NASA.

Simulated Low-Gravity Sloshing in Spherical, Ellipsoidal, and Cylindrical Tanks

FRANKLIN T. DODGE* AND LUIS R. GARZA†
Southwest Research Institute, San Antonio, Texas

Nomenclature

- f_1 = first mode slosh natural frequency
 g = gravity or equivalent linear axial acceleration
 N_{Bo} = Bond number, $\rho g R_o^2 / \sigma$
 R_o = radius of tank
 ν, ρ = liquid kinematic viscosity and density
 σ = surface tension

Introduction

SINCE the primary effect of reduced gravity on propellant sloshing is to accentuate the surface tension forces relative to the gravity forces in the body of the liquid, the Bond num-

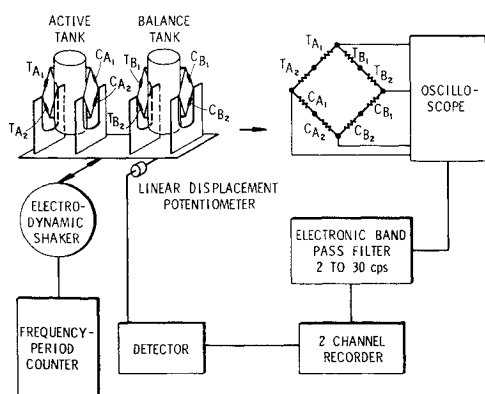


Fig. 1 Schematic of slosh-force dynamometer.

Presented as Paper 69-1004 at the AIAA/ASTM/IES 4th Space Simulation Conference, Los Angeles, Calif., September 8-10, 1969; submitted September 9, 1969; revision received October 24, 1969. Research sponsored by NASA-MSC Contract NAS8-20290; this Note is a condensation of Technical Reports 6 and 7. The authors express their thanks to G. L. Dugger for his aid in editing the manuscript.

*Senior Research Engineer, Department of Mechanical Sciences. Member AIAA.

†Senior Research Engineer, Department of Mechanical Sciences.

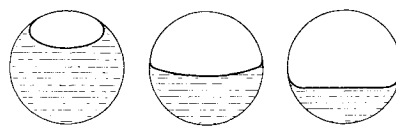


Fig. 2 Change in free-surface curvature with filling level, for equal bond numbers.

ber, $N_{Bo} = \rho g R_o^2 / \sigma$, which is a measure of these two forces, is the correct indicator of "low-gravity" simulation. ($N_{Bo} = 0$ indicates zero gravity, but $N_{Bo} = 40$ is typical for large boosters even when gravity is only 10^{-5} of earth gravity.) Also, for $N_{Bo} < 100$ simulations, the correct static contact angle of the free surface at the tank walls must be duplicated and contact angle "hysteresis" or "dynamic contact angle" accounted for.

Several methods of simulating low gravity using scale models have been advanced. In a *drop-tower*, the effective gravity acting on the liquid is reduced by allowing the experimental package to fall freely, see Ref. 1. In the *magneto-hydrodynamic* method, body forces generated in an electrically conducting liquid by crossed electric and magnetic fields are used to cancel gravity.² The *dielectrophoretic* method uses a strong electric field and a dielectric liquid to create body forces opposed to gravity.² The *magnetic fluid* method uses a specially prepared magnetic liquid and an axial magnetic field to cancel the gravitational forces.²

Most existing steady-state data have been obtained by using *ultra-small models*, see Ref. 3, since surface tension forces can be increased by decreasing the tank diameter. The two main difficulties of this simulation are 1) the small dynamic slosh force is difficult to measure, and 2) the viscous damping is large compared to the prototype; these difficulties generally limit the simulation to $N_{Bo} > 10$, which, however, still includes most low-gravity missions to date. The data presented in this Note were obtained by this technique, which requires an extremely sensitive and accurate dynamometer-excitation system. (Slosh forces as small as 0.0005 lb had to be measured during tests.) In principle, the dynamometer-excitation package was similar to but much more sensitive than that used for much larger tanks. The force-measuring system is shown schematically in Fig. 1. Each sensing ele-

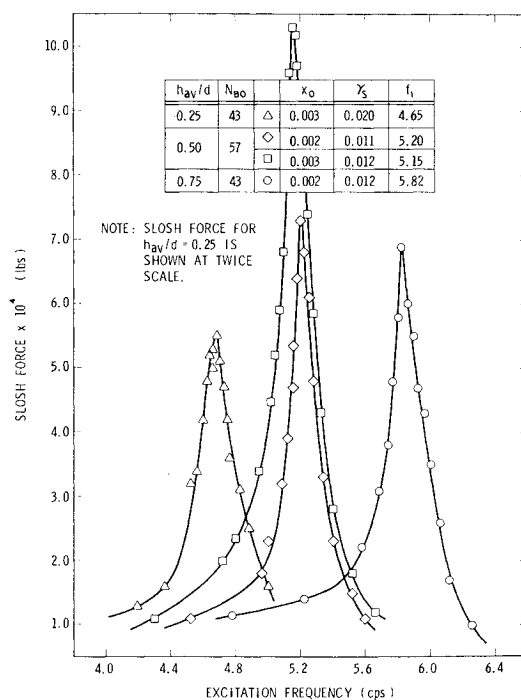


Fig. 3 Typical force response for spherical tanks.

ment (a tension-compression link) had bonded to it a semiconductor strain gage (gage factor = 118), and the test tanks were connected directly to the sensing links. The "active tank" contained the test liquid; a duplicate "balance tank" was used to electrically cancel the inertia signal of the empty active tank in a Wheatstone bridge circuit when both tanks were vibrated at the same frequency and amplitude. Thus, during sloshing, the signal recorded was due solely to the sloshing pressures on the tank walls. This procedure improved the sensitivity of the apparatus so greatly that the entire apparatus had to be covered to prevent stray air currents from impinging on the tank and overwhelming the slosh signal.

All the tanks were carefully cleaned before using. Triply distilled water was first used as the test liquid, because of water's high ratio of surface tension to density. But no matter how careful the cleaning, the water's free surface would soon "stick" to the tank walls, and most of the wave action would cease. Since the liquid sliding freely up and down the tank walls (the "free-edge" condition) is the practical case, the tests with water were abandoned and reagent-grade methanol, acetone, and carbon tetrachloride, which are all good cleaners, were used instead; all these liquids had a 0° static contact angle, and no "hysteresis" effects were evident.

By analyzing the errors and inaccuracies in the apparatus and test procedure, the slosh force data were estimated to be within $\pm 5\%$ of their true values.⁴

Test Results

The three experimental objectives were the determination of 1) slosh force amplitude as a function of lateral excitation 2) resonant slosh frequency, and 3) slosh damping. Four tank geometries were employed: flat-bottomed cylindrical (diameters of 1.36, 1.04, 0.688, and 0.383 in.); spherical (diameters of 1.36 and 1.04 in.); and two kinds of oblate ellipsoidal, one having a major-to-minor axis ratio of $(2)^{1/2}/1.0$ (major diameters of 1.354 and 0.760 in.) and the other having a ratio of 1.99/1.0 (the same major diameters). Besides tank geometry, the variables included ρ , σ , ν , and liquid filling level, which thus varied N_{BO} and the Galileo number, $N_{GA} = R_o^{3/2} g^{1/2}/\nu$, the form of Reynolds number pertinent to sloshing.

Cylindrical tanks

These results have been presented elsewhere^{4,5} but are reviewed here to point out three important facts. First, the excellent correlation between theory and test helps prove that the simulation method is indeed valid. Secondly, the slosh resonant frequency for $N_{BO} > 10$ is not a strong function of

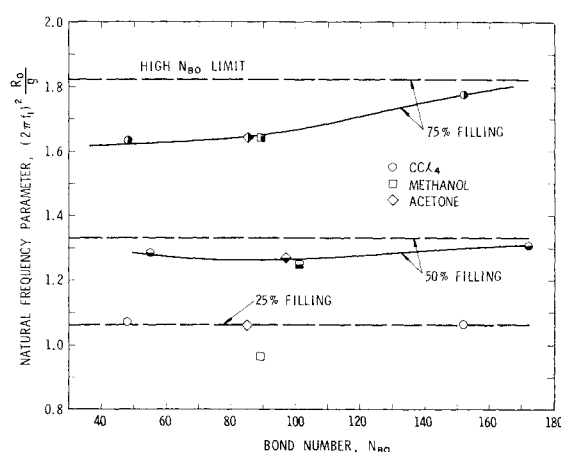


Fig. 5 Variation of natural frequency with bond number for $(2)^{1/2}/1.0$ ellipsoidal tanks.

N_{BO} : the maximum variation in $(2\pi f_1)^2 R_o/g$ is no more than about 10% from $N_{BO} = \infty$ to $N_{BO} = 10$. Thirdly, the slosh damping coefficient, γ_s , depends on both N_{BO} and N_{GA} for $N_{BO} < 100$. The kind of correlation that fits the data best is $\gamma_s = 0.83 N_{GA}^{-1/2} (1 + 8.2 N_{BO}^{-3/5})$, and this correlation reduces to the correct form as $N_{BO} \rightarrow \infty$. The γ_s results compare very well to drop tower results,¹ which also show that the preceding correlation is not valid when $N_{BO} < 3$.

Spherical tanks

The N_{BO} range covered in these tests was 43 to 175. Here, N_{BO} is based on the diameter of the liquid free surface, since surface tension forces depend primarily on the free surface size and not on tank size. Liquid filling levels of 15.6, 50.0, and 84.4% of the tank volume were tested, which correspond to an average liquid depth of 25, 50, and 75% of the tank diameter. For the same tank and liquid, N_{BO} for 15.6% and 84.4% filling is the same since the free-surface diameters are the same. Nonetheless, the free surface curvature at the 84.4% filling is much greater, because of the 0° contact angle, as shown in Fig. 2. Thus, identical N_{BO} 's have different effects at different fillings.

Typical curves of force amplitude vs excitation are shown in Fig. 3; note the magnitude of the measured forces. The response is reasonably linear, and the largest forces always occur for a half-full tank. When compared to an existing equivalent (mathematical) mechanical model for infinitely large N_{BO} , using the experimental values of γ_s and f_1 , the experimental peak forces were found to be about 10% smaller than the model predictions, which is also about the discrepancy for cylindrical tanks when going from $N_{BO} = \infty$ to a moderately small N_{BO} .⁴

The difference in natural and resonant frequency is negligible, because of the small damping, and thus the natural frequency can be determined from the force response curves. The resulting variation of $(2\pi f_1)^2 R_o/g$ with N_{BO} and filling level is displayed in Fig. 4. It can be seen that the data points are consistent with each other since, for equal N_{BO} and fill level, the experimental values are the same, regardless of the tank size or liquid properties used. As indicated previously, N_{BO} has a significantly different effect on f_1 at different liquid levels. At low levels, $(2\pi f_1)^2 R_o/g$ is almost independent of N_{BO} , but at the higher levels, it decreases markedly as N_{BO} decreases. This latter change, moreover, is much more pronounced and in the opposite direction than the frequency change in cylindrical tanks. The experimental results compare very well to a recent theory,⁶ which is the solid curve in the figure.

Damping coefficients, computed by the half-bandwidth technique, show that the minimum γ_s occurs for a half-full tank, and that γ_s for the 15.6% filling is about twice that for

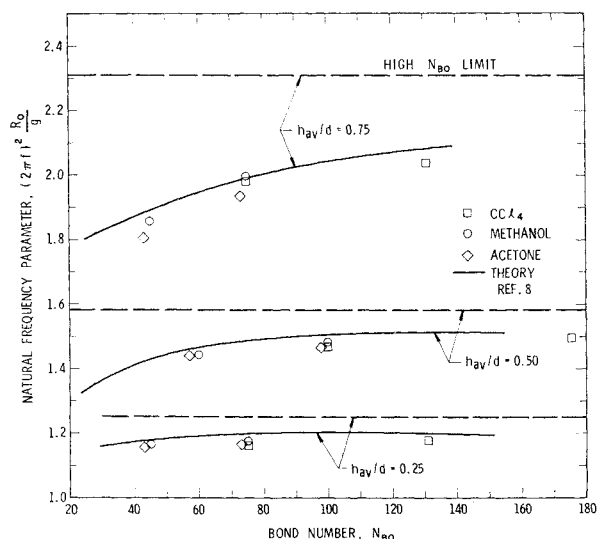


Fig. 4 Variation of natural frequency with bond number for spherical tanks.

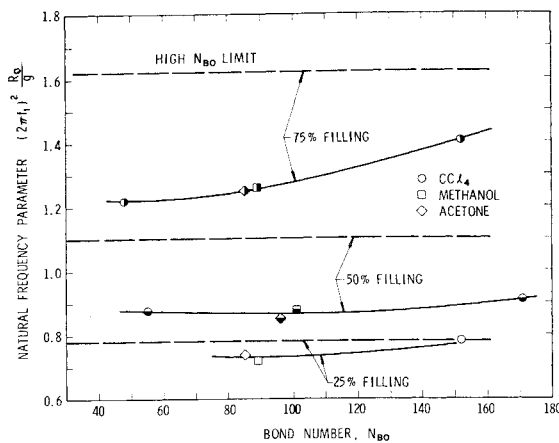


Fig. 6 Variation of natural frequency with Bond number for 1.99/1.0 ellipsoidal tanks.

the 84.4% filling. Similar results hold for large N_{B0} sloshing but, in that case, γ_s for the 15.6 and 84.4% filling are about equal. Thus, once again, the effects of the differences in free surface curvature are evident. Finally, γ_s increases when either N_{GA} or N_{B0} decreases, but an accurate correlation has not yet been obtained.

Ellipsoidal tanks

The N_{B0} range covered in the tests with the oblate ellipsoidal tanks was 48 to 172, based on the free-surface diameter. Liquid filling levels of 25, 50, and 75% of the tank volume were tested; these levels correspond to average liquid depths of 33, 50, and 67% of the minor diameter.

The frequency parameters for the $(2)^{1/2}/1.0$ tank are shown in Fig. 5, and for the 1.99/1.0 tank in Fig. 6. (R_0 used in these figures is one-half the major diameter.) The trends shown are the same observed previously in Fig. 4 for spherical tanks, except that here the difference in free-surface curvature between the low and the high filling level is not so great because of the smaller difference in filling levels. There are no existing low- g slosh theories for ellipsoidal tanks of these eccentricities. Damping results are qualitatively similar to those described for spherical tanks.

Conclusions

The method of ultrasmall model simulation of low-gravity propellant sloshing has been shown to give useful data for the prototype N_{B0} 's greater than about ten. The test results show that N_{B0} influences the slosh natural frequency only slightly for cylindrical tanks, but markedly for spherical and ellipsoidal tanks that are over half full. The slosh damping has also been shown to depend upon N_{B0} . Finally, qualitative determinations of the "slosh mass" in an equivalent mechanical model indicate that the amount of liquid participating in the sloshing motion is less than for the corresponding large N_{B0} , flat interface case.

References

- Salzman, J. A., Labus, T. L., and Masica, W. J., "An Experimental Investigation of the Frequency and Viscous Damping of Liquids During Weightlessness," TN D-4132, 1967, NASA.
- Dodge, F. T., "A Discussion of Laboratory Methods of Simulating Low-Gravity Fluid Mechanics," TR 3, Contract NAS8-20290, 1967, Southwest Research Institute, San Antonio, Texas.
- Satterlee, H. M. and Reynolds, W. C., "The Dynamics of the Free Liquid Surface in Cylindrical Containers Under Strong Capillary and Weak Gravity Conditions," TR IG-2, 1964, Dept. of Mechanical Engineering, Stanford Univ.
- Dodge, F. T. and Garza, L. R., "Experimental and Theoretical Studies of Liquid Sloshing at Simulated Low Gravity," *Transactions of the ASME, Journal of Applied Mechanics*, Vol. 34, Sept. 1967, pp. 555-562.

⁵ Dodge, F. T. and Garza, L. R., "Simulated Low-Gravity Sloshing in Cylindrical Tanks Including Effects of Damping and Small Liquid Depth," *Proceedings of 1968 Heat Transfer and Fluid Mechanics Institute*, Stanford Univ. Press, 1968, pp. 67-76.

⁶ Concus, P., Crane, G. E., and Satterlee, H. M., "Small Amplitude Lateral Sloshing in Spheroidal Containers Under Low Gravitational Conditions," Final Report, Contract NAS3-9704, 1969, Lockheed Missiles & Space Corp., Sunnyvale, Calif.

Use of a Polynomial Force Model to Supplement a Reduced Gravity Model

ROBERT H. GERSTEN* AND NORMAN S. HALL†
Aerospace Corporation, El Segundo, Calif.

IN a previous publication¹ the authors presented a polynomial force model to supplement the conventional spherical harmonics representation of the terrestrial gravitational field for the determination of near-equatorial, near-synchronous, near-circular satellite orbits. The present paper extends this analysis to a consideration of the orbit determination accuracy attainable when the polynomial force model is used to supplement a gravity model consisting only of μ and J_2 terms.

Discussion

The approach taken in Ref. 1 was to supplement the conventional spherical harmonics representation of the terrestrial gravity field with a forcing function with (radial, along-track, and cross-track) components represented by polynomials p_i of the form

$$p_i = a_{i1} + a_{i2}(r - r_0) + a_{i3}(\phi - \phi_0) + a_{i4}(\lambda - \lambda_0)$$

where ϕ = vehicular sublatitude, λ = vehicular sublongitude, r = vehicular separation from the geocenter, $i = 1, 3$ for radial, in-track and cross-track components, a_{ij} = constant coefficients, and 0 = subscript notation for nominal value. One then solves for the a_{ij} in the same manner as one determines the spherical harmonics of ever increasing degree in a conventional representation of the earth's gravity field.

The "data" utilized were generated from a simulation using an eighth-degree, eighth-order (8/8) model of the earth's gravity field. The "measurements" were taken over a duration of 20 days and consisted of nonsynoptic range measurements originating from tracking stations located in Calif., New England, and Hawaii supplemented by angular "data" originating from eight other stations. The range data were taken at a sampling rate of one observation every 8 sec over 5-min intervals, these latter intervals being separated by 10 hr. The angular data were sampled at a rate of one observation every 24 hr. One-sigma tracking errors were assumed to be 50 ft due to bias and 60 ft due to noise in the range measurements, and 2 arcsec due to noise and bias in the angular measurements. These latter values are considered

Table 1 Optimistic and pessimistic estimates of gravity model errors

Coefficient	μ	J_2	J_3	J_4	J_{22}	J_{31}
Optimistic error, %	0.001	0.02	10	10	10	10
Pessimistic error, %	0.01	0.2	100	100	100	100

Received September 9, 1969; revision received October 13, 1969.

* Member of the Technical Staff. Member AIAA.

† Member of the Technical Staff.